RESEARCH ARTICLE

In Silico Analysis of 2,4-Thiazolidinedione Derivatives as Potential Insulin Sensitizers for the Treatment of Diabetes Mellitus

Jain Usha N[1,2*], Jain Nitin P[2], Amrutkar Sunil V[1]

[1]*Department of Pharmaceutical Chemistry, GES's Sir Dr. M. S. Gosavi College of Pharmaceutical Research and Education, Nashik, Maharashtra-422002, India*
[2]*Department of Pharmaceutical Chemistry, RJS College of Pharmacy, Kopargaon, Ahilyanagar Maharashtra-423601, India*

Received: 13th Sep, 2024; Revised: 30th Oct, 2024; Accepted: 14th Nov, 2024; Available Online: 25th Dec, 2024

ABSTRACT
This study explores the design and evaluation of 2,4-thiazolidinedione (TZD) compounds as potential antidiabetic candidate through in silico methods. A total of 22 TZD derivatives were virtually designed, assessed for synthetic accessibility, and analyzed for ADME properties using Maestro 24.3. Molecular docking studies against the PPARδ receptor (PDB ID: 5Y2O) identified B-TZD11 and B-TZD13 as the most promising candidates, exhibiting strong binding interactions. Toxicity predictions using Protox-III indicated moderate toxicity (Class 4), with some compounds showing nephrotoxicity and BBB penetration. The derivatives demonstrated favorable pharmacokinetic properties, including high oral absorption and metabolic stability. Computational studies indicate that these compounds may act as insulin sensitizers, but further biological testing is needed to assess their effectiveness and potential risks. This study supports the development of innovative antidiabetic agents with improved therapeutic benefits.
Keywords: Thiazolidinedione, PPAR$_\delta$, Anti-diabetic, Molecular docking, Insulin sensitizer.
How to cite this article: Jain Usha N, Jain Nitin P, Amrutkar Sunil V. In *Silico* Analysis of 2,4-Thiazolidinedione Derivatives as Potential Insulin Sensitizers for the Treatment of Diabetes Mellitus. International Journal of Pharmaceutical Quality Assurance. 2024;15(4):2455-72. doi: 10.25258/ijpqa.15.4.46
Source of support: Nil.
Conflict of interest: None

INTRODUCTION

Type 2 diabetes majorly observed in old age people due to lack of activity, obese person due to lack of exercise and family history. Pancreas secrete sufficient insulin but body cell cannot utilize effectively and develop resistance. Obesity is the primary cause of insulin resistance.[1] Thiazolidinedione act as insulin sensitizer through activation of PPAR$_\delta$. PPAR$_\delta$ present in white adipocytes tissue and muscle.[2,3] Pioglitazone and rosiglitazone thiazolidinedione drugs (Fig 1) use for the treatment and management of diabetes mellitus shown in.[4,5] These drugs have side effect liver damage, bladder cancer and for this reason limited uses of this class of drug. Consequently, there is a need of effective and safe insulin sensitizer.[6,7]

We design 22 derivatives by condensation of acetamide at nitrogen to thiazolidinedione moiety. For the understating the molecular interaction at molecule level of cell for the treatment of diabetes mellitus carried out the research in search of novel insulin sensitizer. This research included molecular docking evaluation, toxicity predication, drug likeness and ADME determination which contribute for prediction of potential of PPAR$_\delta$ activator for the diabetes mellitus treatment. Targeting the PPAR$_\delta$ is the challenging to develop the safe antihyperglycemic agent.[8] The research on 2,4-TZD as an effective insulin sensitizer in managing diabetic mellitus in obese person to provide potential insight, combining the molecular docking studies, Lipinski rule drug likeness, prediction of toxicity and ADME analysis to identify molecule having effective drug-receptor interaction and favourable drugs likeness. Modern technology software including Maestro 24.3 and protox III use for the molecular docking study, ADME predication, drug likeness and toxicity prediction of design molecule.[9,10]

Experimental Design of 2,4-Thiazolidinedione Derivatives

In the present research, the design of 2,4-thiazolidinedione (TZD) derivatives for antidiabetic activity was guided by a comprehensive review of the literature and databases. The priority in selecting the scaffolds was to focus on structures with established antidiabetic activity that could be synthesized using straight forward and well-documented experimental procedures. A total of 22 molecules were virtually designed based on these criteria and subjected to *in-silico analysis* to evaluate their potential as antidiabetic agents. The design process emphasized structural modifications at specific positions of the TZD moiety, particularly substitutions at the nitrogen atom, to enhance biological activity and pharmacokinetic properties.[11]

Synthetic Accessibility (SA) Assay

SA is a critcal factor in organic chemistry, especially in drug synthesis and process development. It evaluates how easily and efficiently a molecule can be synthesized in a laboratory setting, providing insight into the practical

**Author for Correspondence: unjain11@gmail.com*

feasibility of manufacturing the compound. In the present study, a synthetic accessibility analysis was performed for 22 compounds of 2,4-thiazolidinedione (TZD) derivatives. The SwissADME server, a widely recognized tool for evaluating molecular properties and drug-likeness, was utilized for this purpose. The SwissADME platform applies computational methods to assess the complexity and synthetic feasibility of the molecules, assigning a score on a scale of 1 to 10.[12]

ADME Analysis and Drug Likeness

To assess the pharmacokinetic properties and pharmaceutical properties of the designed 2,4-thiazolidinedione derivatives, Maestro 24.3 was employed to perform ADME prediction using ligand-based ADME tools. This analysis is crucial for assessing the potential of the molecules to function as drug candidates. Before ADME prediction, all 22 molecules underwent ligand preparation to ensure they were optimized for analysis. This step ensures proper 3D geometry, accurate protonation states, and the assignment of formal charges. The ADME prediction tool was opened in Maestro, and the file containing all ligand entries was selected. The job was executed, and the software computed the ADME-related properties in the background. Once the job was completed, the results were presented in the Project Table, allowing for easy analysis of the predicted properties. These included key parameters such as solubility, permeability, metabolic stability, and lipophilicity. The H-bond assignment algorithm was utilized during this process to optimize hydrogen bonding within the ligands. This step ensures the stability of the residues, contributing to more reliable predictions of molecular interactions and stability.[13–16]

Table 1: Structure of designed 2,4-thiazolidinedione derivatives and their synthetic accessibility

Compd	Structure	Synthetic Accessibility	Compd	Structure	Synthetic Accessibility
B-TZD1	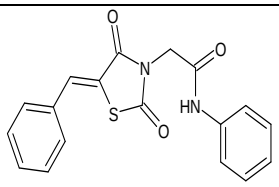	3.35	B-TZD12	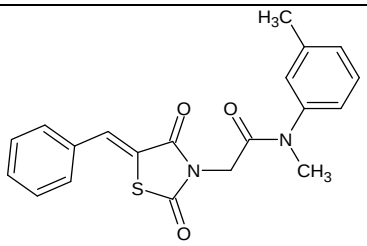	3.56
B-TZD2	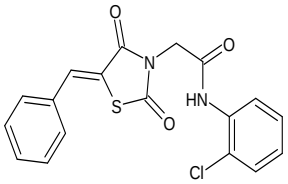	3.35	B-TZD13	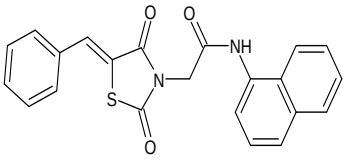	3.57
B-TZD3	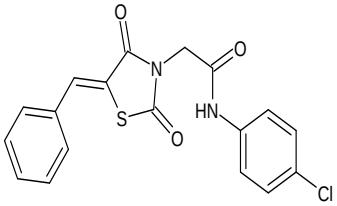	3.32	B-TZD14	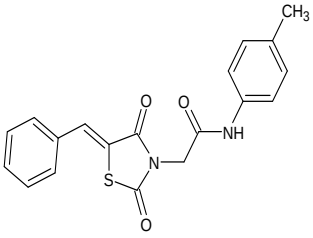	3.45
B-TZD4	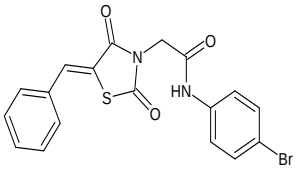	3.37	B-TZD15	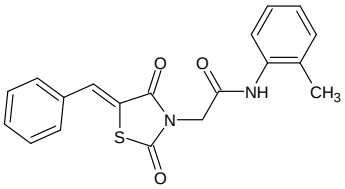	3.45
B-TZD5	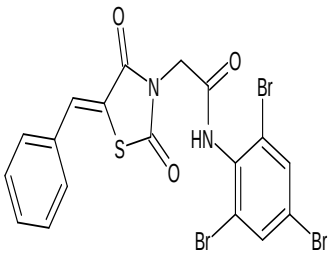	3.40	B-TZD16	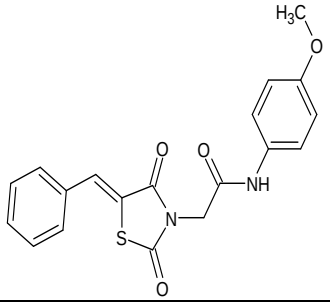	3.40

Table 1: Structure of designed 2,4-thiazolidinedione derivatives and their synthetic accessibility

Compd	Structure	Synthetic Accessibility	Compd	Structure	Synthetic Accessibility
B-TZD6	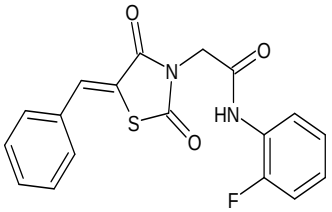	3.35	BTZD17	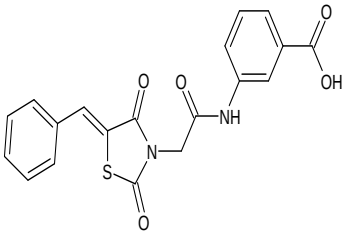	3.39
B-TZD7	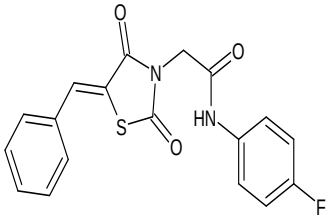	3.31	B-TZD18	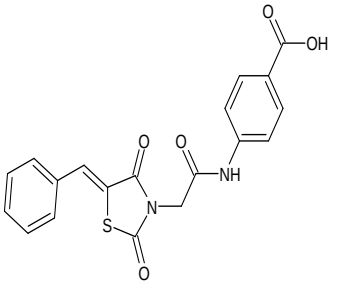	3.36
B-TZD8	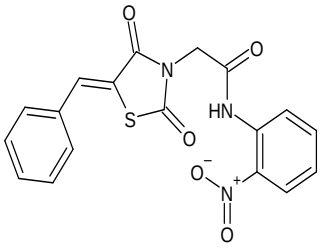	3.56	B-TZD19	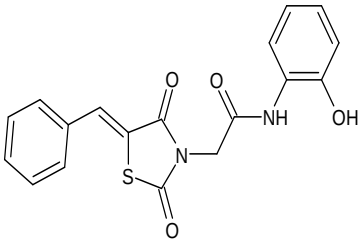	3.35
B-TZD9	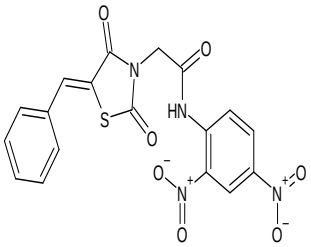	3.71	B-TZD20	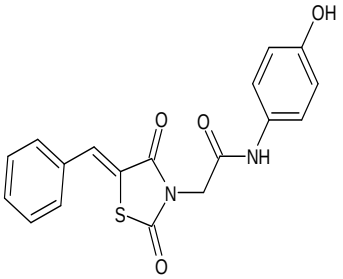	3.34
B-TZD10	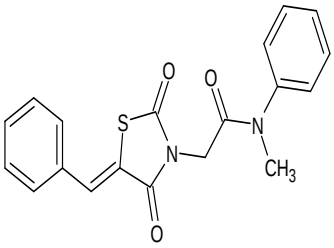	3.46	B-TZD21	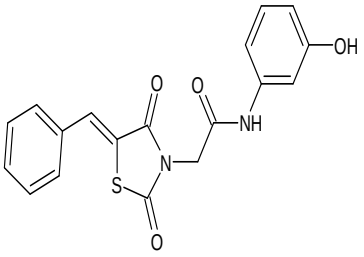	3.38
B-TZD11	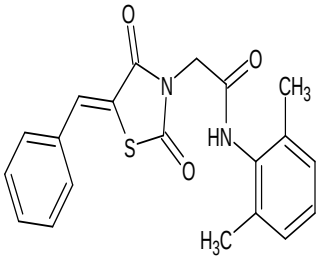	3.54	B-TZD22	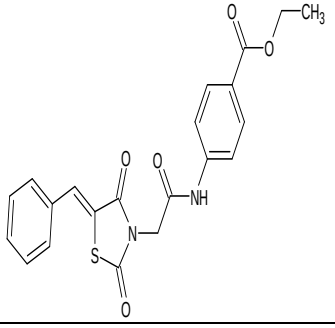	3.57

Table 2: *In-silico* Predicted ADME analysis of 2,4-thiazolidinedione derivatives

	Absorption	Distribution		Metabolism	Excretion
Molecule	%Human Oral Absorption	QPlogPo/w	QPlogBB	#metab	QPlogS
Pioglitazone	100	3.548	-0.87	5	-4.299
B- TZD 01	95.485	3.144	-0.949	2	-4.706
B- TZD 02	100	3.822	-0.811	2	-5.67
B- TZD 03	100	3.861	-0.801	1	-5.713
B- TZD 04	100	3.937	-0.794	1	-5.826
B- TZD 05	95.364	4.961	-0.348	1	-6.909
B- TZD 06	100	3.585	-0.849	2	-5.283
B- TZD 07	100	3.604	-0.844	1	-5.339
B- TZD 08	84.736	2.827	-1.462	3	-4.495
B- TZD 09	51.063	2.117	-2.572	3	-4.635
B- TZD 10	100	3.464	-0.769	2	-4.512
B- TZD 11	100	3.997	-0.681	4	-5.397
B- TZD 12	100	3.708	-0.831	3	-5.062
B- TZD 13	100	4.319	-0.937	1	-6.063
B- TZD 14	100	3.652	-0.952	2	-5.463
B- TZD 15	100	3.588	-0.716	3	-4.97
B- TZD 16	100	3.465	-1.047	2	-5.207
B- TZD 17	63.829	2.664	-1.198	2	-4.922
B- TZD 18	64.448	2.678	-1.144	1	-4.864
B- TZD 19	85.188	2.699	-1.469	3	-4.658
B- TZD 20	83.798	2.667	-1.556	2	-4.726
B- TZD 21	83.853	2.668	-1.551	3	-4.719
B- TZD 22	88.338	3.512	-1.856	1	-6.184

Table 3: Drug likeness prediction by Lipinski's rule of five of 2,4-thiazolidinedione derivatives

Molecule	Mol_MW	QPlogPo/w	DonorHB	AccptHB	Violence of Lipinski's rule	Rule of Three
Pioglitazone	357.426	3.548	1	5.25	0	0
B- TZD 01	338.38	3.144	1	5.5	0	0
B- TZD 02	372.825	3.822	1	5.5	0	0
B- TZD 03	372.825	3.861	1	5.5	0	1
B- TZD 04	417.276	3.937	1	5.5	0	1
B- TZD 05	575.068	4.961	1	5.5	1	1
B- TZD 06	356.371	3.585	1	5.5	0	0
B- TZD 07	356.371	3.604	1	5.5	0	0
B- TZD 08	383.378	2.827	1	6.5	0	0
B- TZD 09	428.375	2.117	1	7.5	1	0
B- TZD 10	352.407	3.464	0	6	0	0
B- TZD 11	366.434	3.997	1	5.5	0	0
B- TZD 12	366.434	3.708	0	6	0	0
B- TZD 13	388.44	4.319	1	5.5	0	1
B- TZD 14	352.407	3.652	1	5.5	0	0
B- TZD 15	352.407	3.588	1	5.5	0	0
B- TZD 16	368.406	3.465	1	6.25	0	0
B- TZD 17	382.39	2.664	2	7.5	0	1
B- TZD 18	382.39	2.678	2	7.5	0	1
B- TZD 19	354.38	2.699	2	6.25	0	0
B- TZD 20	354.38	2.667	2	6.25	0	0
B- TZD 21	354.38	2.668	2	6.25	0	0
B- TZD 22	410.444	3.512	1	7.5	0	1

Table 4: Molecular Docking score and parameter contribute for the docking score of compounds using the p5 (PDB Id-5Y2O) downloaded from the PDB.

Compound	G Score	Docking score	Electro	H Bond	Lipophilic	Low M.W.
Pioglitazone	-10.731	-10.282	-0.435	-1.799	-6.903	-0.312
B- TZD 11	-9.309	-9.309	-0.031	-0.562	-6.432	-0.279
B- TZD 13	-9.226	-9.226	-0.008	-0.592	-6.614	-0.205

Table 4: Molecular Docking score and parameter contribute for the docking score of compounds using the p5 (PDB Id-5Y2O) downloaded from the PDB.

Compound	G Score	Docking score	Electro	H Bond	Lipophilic	Low M.W.
B- TZD 09	-8.555	-8.555	-0.047	-0.586	-6.19	-0.072
B- TZD 15	-8.324	-8.324	-0.06	-0.592	-5.759	-0.325
B- TZD 18	-8.022	-8.021	-0.379	-0.457	-5.904	-0.229
B- TZD 02	-7.974	-7.974	-0.102	-0.581	-5.277	-0.257
B- TZD 16	-7.502	-7.502	-0.094	-0.739	-5.74	-0.272
B- TZD 19	-7.394	-7.393	-0.311	-1.495	-4.583	-0.319
B- TZD 12	-6.761	-6.761	-0.083	-0.562	-5.175	-0.279
B- TZD 20	-6.675	-6.675	-0.162	-0.83	-5.274	-0.319
B- TZD 06	-6.641	-6.641	-0.036	-0.571	-4.726	-0.312
B- TZD 05	-6.562	-6.562	-0.056	-0.494	-5.027	0
B- TZD 10	-6.493	-6.493	-0.07	-0.553	-4.901	-0.325
B- TZD 03	-6.488	-6.488	-0.013	-0.55	-4.913	-0.257
B- TZD 01	-6.486	-6.486	-0.052	-0.561	-4.789	-0.372
B- TZD 17	-6.422	-6.422	-0.238	-0.78	-5.366	-0.229
B- TZD 22	-6.397	-6.397	-0.218	-0.127	-5.895	-0.132
B- TZD 07	-6.397	-6.397	-0.045	-0.558	-4.624	-0.312
B- TZD 14	-6.397	-6.397	-0.074	-0.57	-4.778	-0.325
B- TZD 21	-6.393	-6.391	-0.07	-0.564	-4.768	-0.319
B- TZD 04	-6.376	-6.376	-0.019	-0.565	-4.896	-0.109
B- TZD 08	-6.207	-6.207	-0.125	-0.639	-4.482	-0.222

Table 5: Molecular Docking binding Interaction results assay of 2,4-thiazolidionedione derivatives with $PPAR_{\delta}$

Compound	Binding affinity	Interacting residues	Type of Interaction
BTZD-1	-6.486	ILE326, MET329, LEU330, LEU333, VAL339, LEU340, ILE341, MET348, LEU255, ILE281, ILE296, ALA292	Hydrophobic Interaction
		ARG288	Charge +ve
		SER289, SER342	Polar Interaction
		CYS285	H-Bond
BTZD-2	-7.974	TYR473, ILE326, TYR327, LFU330, LEU333, VAL339, LEU340, ILE341, ILE281, PHE363, MET364, MET348	Hydrophobic Interaction
		CYS285	H-Bond
		SER289, HIE449, SER342, HIE323	Polar Interaction
		ARG288	Charge +ve
BTZD-3	-6.488	ALA29, ILE326, MET329, LEU330, LEU333, VAL339, LEU340, ILE341, MET348, ILE281, LEU255, MET364, ILE296	Hydrophobic Interaction
		ARG288	Charge +ve
		SER289, SER342	Polar Interaction
		CYS285	H-Bond
BTZD-4	-6.376	ILE326, MET329, LEU330, LEU333, VAL339, LEU340, ILE341, MET348, LEU255, ILE281, MET364ALA292, ILE296	Hydrophobic Interaction
		GLU259	Charge -ve
		ARG288	Charge +ve
		CYS285	H-Bond
BTZD-5	-6.562	ILE296, MET329, LEU330, LEU333, VAL339, LEU340, ILE341, MET348, ILE281, MET364, ALA292	Hydrophobic Interaction
		ARG288	Charge +ve
		CYS285	H-Bond
		SER342	Halogen Interaction
BTZD-6	-6.641	ILE326, MET329, LEU330, LEU333, VAL339, LEU340, ILE341, MET348, ILE296, ALA292,	Hydrophobic Interaction

Table 5: Molecular Docking binding Interaction results assay of 2,4-thiazolidionedione derivatives with PPAR$_{\delta}$

Compound	Binding affinity	Interacting residues	Type of Interaction
		MET364, LEU255, ILE281	
		ARG288	Charge +ve
		CYS285	H-Bond
		SER342	Polar Interaction
BTZD-7	-6.397	ILE326, MET329, LEU330, LEU333, VAL339, LEU340, ILE341, MET348, LEU255, ILE281, MET364, ILE296	Hydrophobic Interaction
		SER342	Polar Interaction
		ARG288	Charge +ve
		CYS285	H-Bond
BTZD-8	-6.207	ILE326, MET329, LEU330, LEU333, VAL339, LEU340, ILE341, MET348, ILE281, MET364, ALA292, ILE296	Hydrophobic Interaction
		SER342	Polar Interaction
		ARG288	Charge +ve
		CYS285	H-Bond
BTZD-9	-8.555	ILE326, TYR327, LEU330, LEU333, ILE341, LEU340, VAL339, TYR473, PHE363, MET364, MET348, LEU353, ILE281, LEU255	Hydrophobic Interaction
		HIE323, SER289, GLN286, SER342	Polar Interaction
		CYS285	H-Bond
		HIE	Pi-Pi Interaction
		ARG288	Charge +ve
BTZD-10	-6.493	ALA292, ILE326, MET329, LEU330, VAL339, LEU340, ILE341, LEU353, MET348, LEU255, ILE249, ILE281, MET364, PHE363, ILE296	Hydrophobic Interaction
		SER342	Polar Interaction
		ARG288	Charge +ve
		CYS285	H-Bond
BTZD-11	-9.309	ILE326, TYR327, LEU330, LEU333, ILE341, LEU340, VAL339, PHE363, MET364, MET348, LEU353	Hydrophobic Interaction
		HIE323, SER289, GLN286, SER342	Polar Interaction
		ARG288	Charge +ve
		HIE449	Pi-Pi Interaction
		CYS285	H-Bond
BTZD-12	-6.761	ILE326, ILE296, MET329, LEU330, LEU333, VAL339, LEU340, ILE341, ILE249, LEU255, ILE281, MET348, LEU353, MET364, PHE363	Hydrophobic Interaction
		ARG288	Charge +ve
		CYS285	H-Bond
		SER342	Polar Interaction
BTZD-13	-9.226	ILE326, TYR327, LEU330, LEU333, VAL339, LEU340, ILE341, ILE281, MET348, LEV353, PHE363, MET364, TYR473	Hydrophobic Interaction
		HIE323, SER289, SER342	Polar Interaction
		ARG288	Charge +ve
		CYS285	H-Bond
		HIE449	Pi-Pi Interaction
BTZD-14	-6.397	ILE326, MET329, LEU330, LEU333, VAL339.LEU340, HLE341, MET348, LEU255, ALA292, MET364	Hydrophobic Interaction
		ARG288	Charge +ve
		CYS285	H-Bond
BTZD-15	-8.324	TYR473, ILE326, TYR32, LEU330, LEU333, VAL339, LEU340, ILE341, ILE281, PHE363, MET364, MET348, LEU353	Hydrophobic Interaction
		HLE323, SER289, SER342	Polar Interaction

Table 5: Molecular Docking binding Interaction results assay of 2,4-thiazolidionedione derivatives with $PPAR_{\delta}$

Compound	Binding affinity	Interacting residues	Type of Interaction
		CYS	H-Bond
		ARG288	Charge +ve
		HLE449	
BTZD-16	-7.502	ILE326, LEU330, MET364, PHE363, CYS285, ILE281, LEU255, LEU353, MET348, ILE341, LEU340, VAL339, TYR473	Hydrophobic Interaction
		CYS367, ARG288, ARG280	Charge +ve
		TYR327	H-Bond
		HLE449, SER289	Polar Interaction
		GLU259	
BTZD-17	-6.422	MET364, PHE363, LEU330, ILE326, ALA292, CYS285, LEU353, VAL339, LEU340, ILE341, LEU255	Hydrophobic Interaction
		TYR327	H-Bond
		CYS367, ARG280, ARG288	Charge +ve
		GLU259	
BTZD-18	-8.021	TYR473, ILE326, TYR327, LEU330, LEU333, VAL339, LEU340, ILE341, ILE281, CYS285, LEU255, MET348, PHE363, MET364	Hydrophobic Interaction
		HIE323, SER289, HIE449, SER342	Polar Interaction
		TYR327, SER289, CYS285	H-Bond
		GLU259	Charge -ve
		ARG288, LYS367	Charge +ve
BTZD-19	-7.393	LEU255, ILE281, MET348, CYS285, MET364, ALA292, ILE326, ILE296, MET329, LEU330, VAL339, LEU333, LEU340, ILE341	Hydrophobic Interaction
		SER342, SER289	Polar Interaction
		ARG288	Charge +ve
		GLY284, CYS285	H-Bond
		ARG288	Pi-Pi Interaction
		GLY284	Glycine
BTZD-20	-6.675	LEU255, ILE281, CYS285, ILE341, LEU340, VAL339, ILE326, TYR327, LEU330, MET348, MET364, PHE363	Hydrophobic Interaction
		HIE323, SER289, SER342	Polar Interaction
		GLU259	Charge -ve
		LYS367, ARG288, ARG280	Charge +ve
		SER342, TYR327	H-Bond
		GLY284	Glycine
BTZD-21	-6.391	ILE281, CYS285, MET364, ALA292, ILE326, ILE296, MET329, LEU330, LEU333, VAL339, LEU340, ILE341, MET348, LEU255	Hydrophobic Interaction
		SER342	Polar Interaction
		ARG288	Charge +ve
		CYS285	H-Bond
		ARG288	Pi-Pi Interaction
BTZD-22	-6.397	ILE281,,PHE282,CYS285, TYR473, LEU453, LEU465, LEU469, ILE326, TYR327, LEU330, MET364, PHE363, VAL339, LEU340, ILE341, LEU353,MET348	Hydrophobic Interaction
		HIE323, HIE449, SER289, GLN286, SER342	Polar Interaction
		GLU259	Charge -ve
		LYS367,ARG288,ARG280	Charge +ve
		GLY284	Glycine

Table 6: Predicted Toxicity of designed molecule of 2,4-thiazolidinedione derivatives

Compound	Predicted toxicity class	Predicted LD_{50} (mg/Kg)	Organ toxicity			End point toxicity	
			Hepato-toxicity	Nephro-toxicity	Cardio-toxicity	Active for	Inactive for
BTZD-1	4	1000	Inactive	Active	Inactive	BBB-Barrier	Mutagenicity, Immunotoxicity, cytotoxicity and carcinogenicity
BTZD-2	4	1313	Inactive	Inactive	Inactive	BBB-Barrier	Mutagenicity, Immunotoxicity, cytotoxicity and carcinogenicity
BTZD-3	4	1313	Inactive	Inactive	Inactive	BBB-Barrier	Cytotoxicity, Mutagenicity, Immunotoxicity, and carcinogenicity
BTZD-4	4	1000	Inactive	Inactive	Inactive	BBB-Barrier	Carcinogenicity Mutagenicity, Immunotoxicity and cytotoxicity
BTZD-5	4	1000	Inactive	Inactive	Inactive	BBB-Barrier	Mutagenicity, Immunotoxicity, cytotoxicity and carcinogenicity
BTZD-6	4	1000	Inactive	Inactive	Inactive	BBB-Barrier	Cytotoxicity, Mutagenicity, Immunotoxicity, and carcinogenicity
BTZD-7	4	1000	Inactive	Inactive	Inactive	BBB-Barrier	Carcinogenicity Mutagenicity, Immunotoxicity and cytotoxicity
BTZD-8	4	1000	Inactive	Inactive	Inactive	BBB-Barrier, carcinogenicity, Mutagenicity	Cytotoxicity, Immunotoxicity
BTZD-9	4	1000	Inactive	Inactive	Inactive	BBB-Barrier, carcinogenicity, Mutagenicity	Cytotoxicity, Immunotoxicity
BTZD-10	4	1000	Inactive	Inactive	Inactive	BBB-Barrier	Cytotoxicity, Mutagenicity, Immunotoxicity, and carcinogenicity
BTZD-11	4	1000	Inactive	Inactive	Inactive	BBB-Barrier	Carcinogenicity Mutagenicity, Immunotoxicity and cytotoxicity
BTZD-12	4	1000	Inactive	Inactive	Inactive	BBB-Barrier	Cytotoxicity, Mutagenicity, Immunotoxicity, and carcinogenicity
BTZD-13	4	1000	Inactive	Inactive	Inactive	BBB-Barrier	Mutagenicity, Immunotoxicity, cytotoxicity and carcinogenicity
BTZD-14	4	1000	Inactive	Inactive	Inactive	BBB-Barrier	Immunotoxicity, Carcinogenicity Mutagenicity, and cytotoxicity
BTZD-15	4	1000	Inactive	Inactive	Inactive	BBB-Barrier	Immunotoxicity, Carcinogenicity Mutagenicity, and cytotoxicity
BTZD-16	4	1000	Inactive	Inactive	Inactive	BBB-Barrier	Immunotoxicity, Cytotoxicity, carcinogenicity and Mutagenicity
BTZD-17	4	500	Inactive	Active	Inactive	-	BBB-Barrier, Cytotoxicity, Mutagenicity, Immunotoxicity, and carcinogenicity
BTZD-18	4	500	Inactive	Active	Inactive	-	BBB-Barrier, Cytotoxicity, carcinogenicity, Mutagenicity and Immunotoxicity
BTZD-19	4	1000	Inactive	Inactive	Inactive	-	BBB-Barrier, Cytotoxicity,

Table 6: Predicted Toxicity of designed molecule of 2,4-thiazolidinedione derivatives

Compound	Predicted toxicity class	Predicted LD_{50} (mg/Kg)	Organ toxicity			End point toxicity	
			Hepato-toxicity	Nephro-toxicity	Cardio-toxicity	Active for	Inactive for
BTZD-20	4	1000	Inactive	Inactive	Inactive	-	Mutagenicity, Immunotoxicity, and carcinogenicity BBB-Barrier, Cytotoxicity,
BTZD-21	4	1000	Inactive	Active	Inactive	-	Mutagenicity, Immunotoxicity, and carcinogenicity Carcinogenicity
BTZD-22	4	500	Inactive	Active	Inactive	BBB-Barrier	Mutagenicity, Immunotoxicity, cytotoxicity and BBB Barrier Cytotoxicity, Mutagenicity, Immunotoxicity, and carcinogenicity

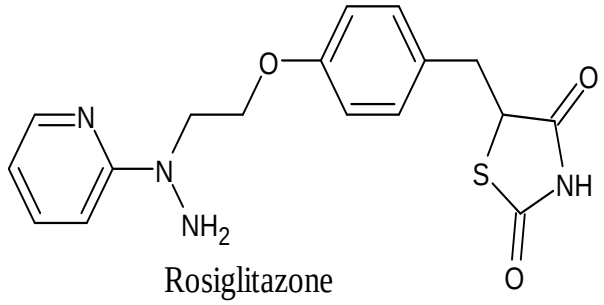

Rosiglitazone

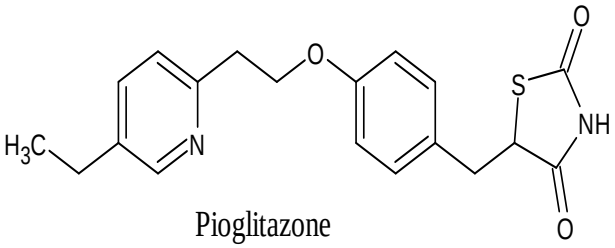

Pioglitazone

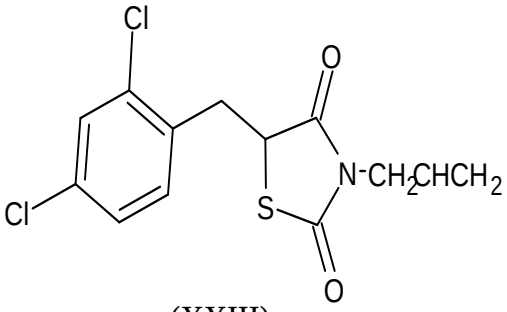

(XXIII)

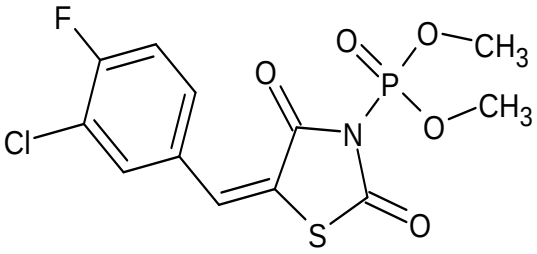

(XXV)

Figure 1: Insulin sensitizer drugs, rosiglitazone and pioglitazone activate the $PPAR_{\delta}$ receptor and Structure of N-protected 2,4-thiazolidinedione having $PPAR_{\delta}$ activator properties

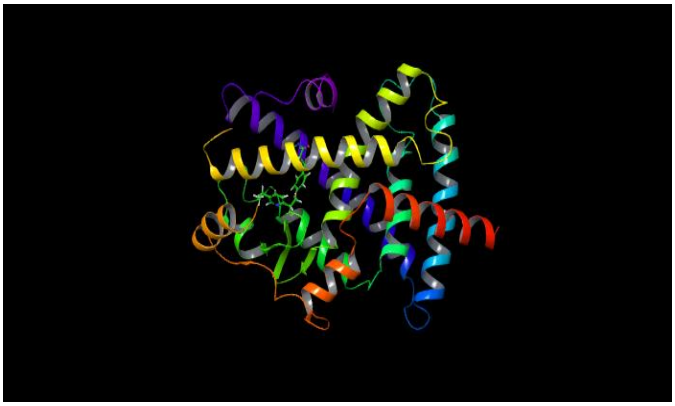

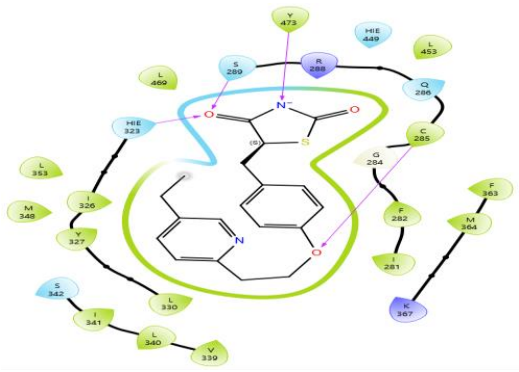

Figure 2: 3D and 2D protein Structure of $PPAR_{\delta}$ (5Y2O) with crystal ligand pioglitazone with amino acid interaction showing

polar interaction with HIE323,S289 and Y473.

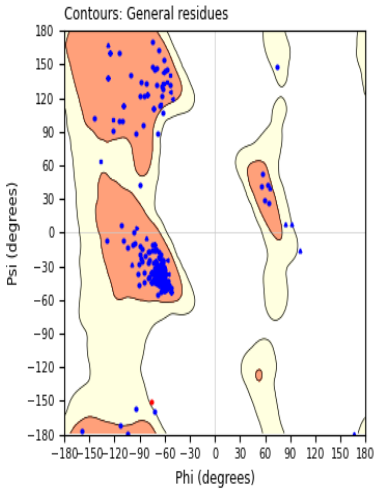

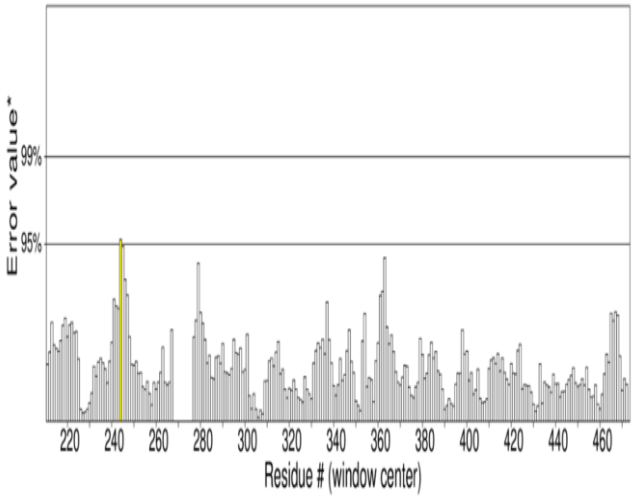

(A) (B)

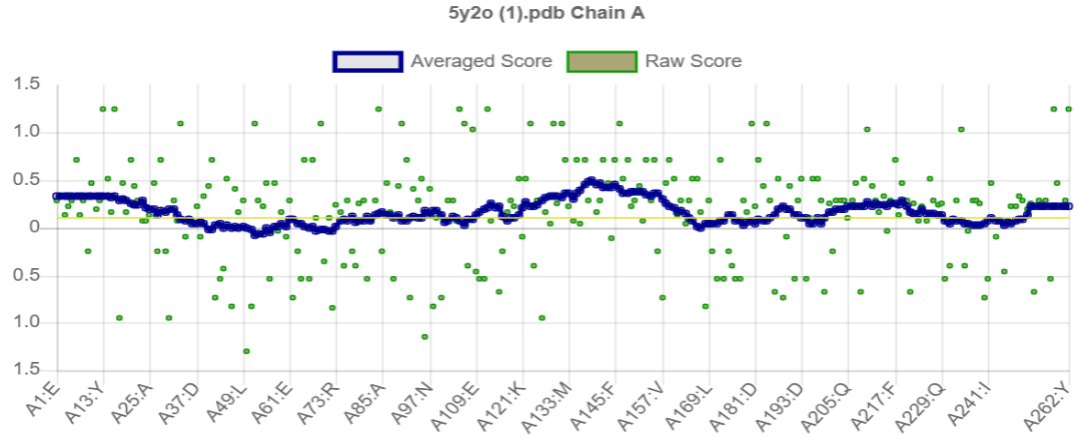

(C)

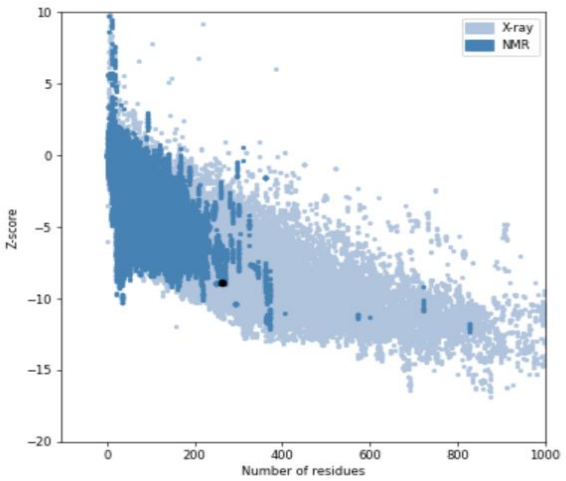

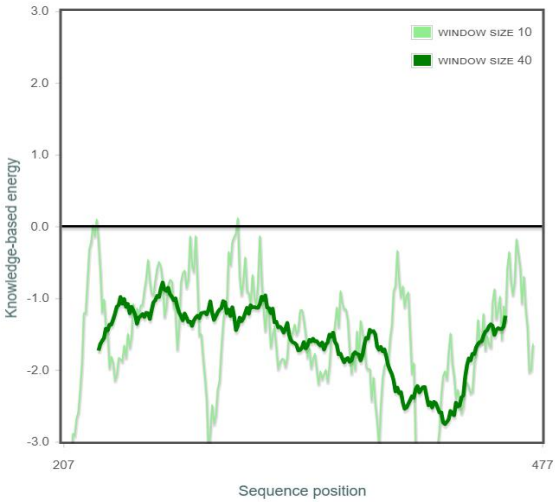

(D)

ERRATA =overall quality factor=98, ProSA chart z-score=-8.89

Figure 3: (A)Ramchandra plot, (B)ERRAT Chart, (C)Verify 3D Chart and (D)ProSA Chart of prepared 5Y2O structure

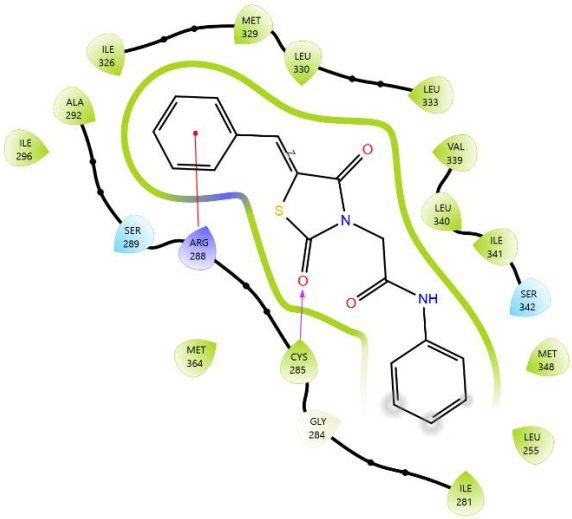

BTZD-1

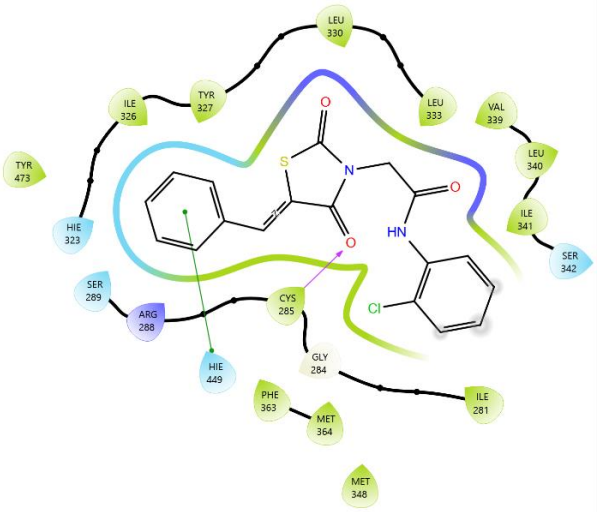

BTZD-2

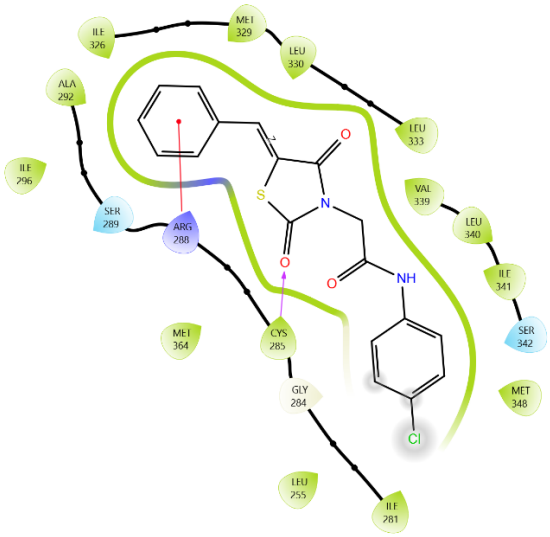

BTZD-3

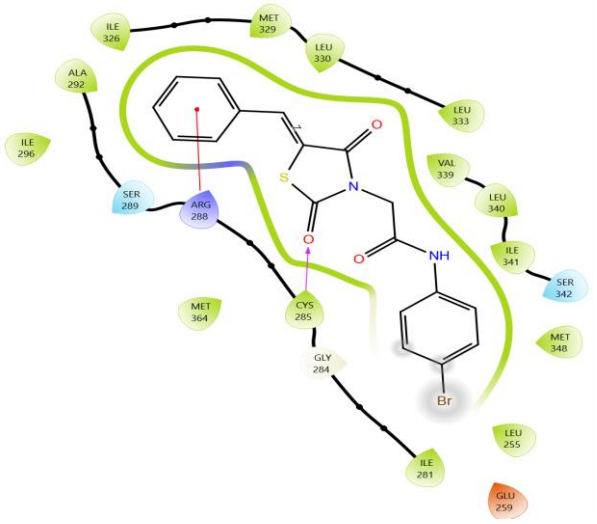

BTZD-4

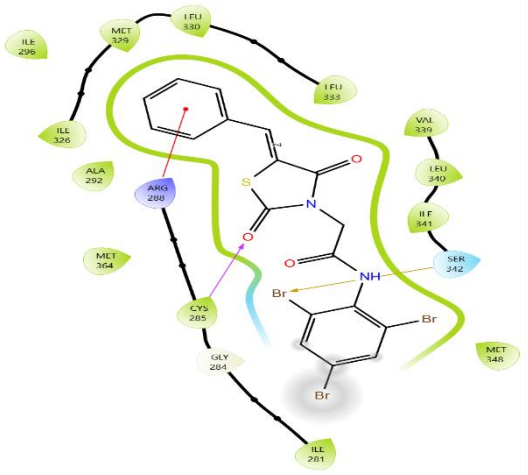

BTZD-5

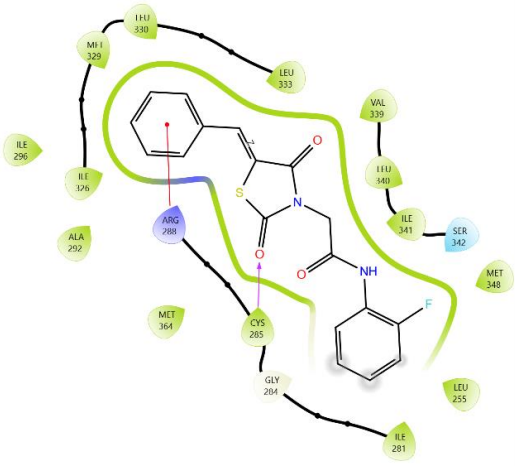

BTZD-6

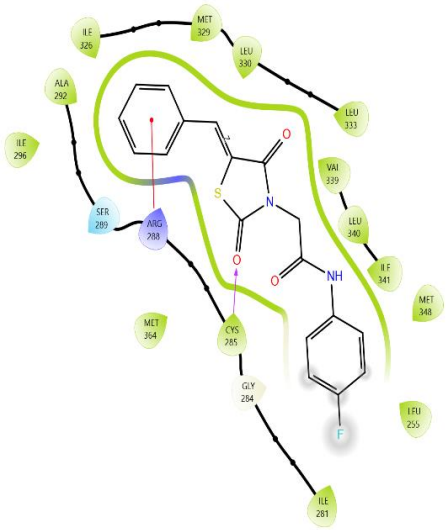

BTZD-7

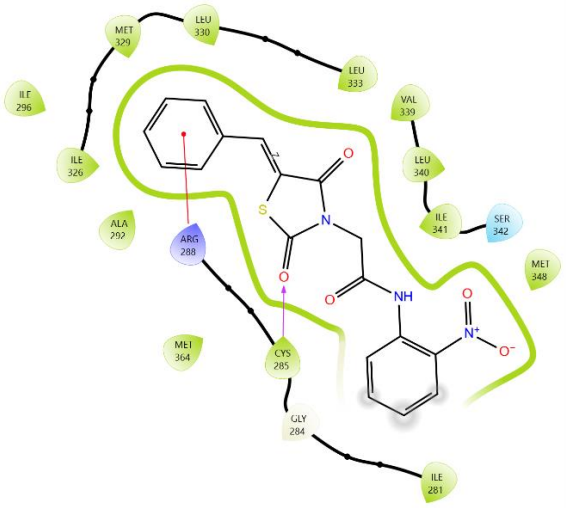

BTZD-8

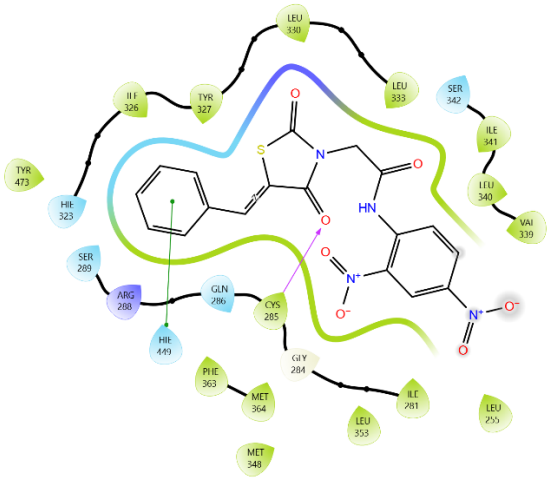

BTZD-9

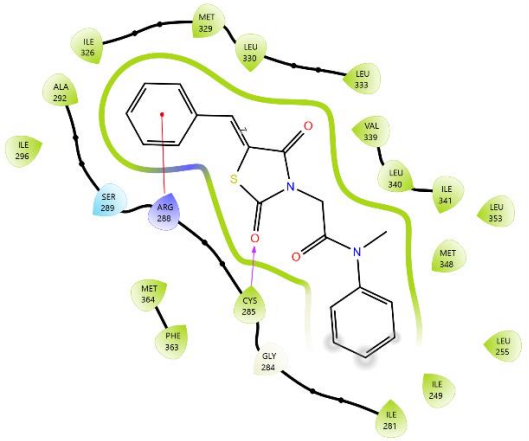

BTZD-10

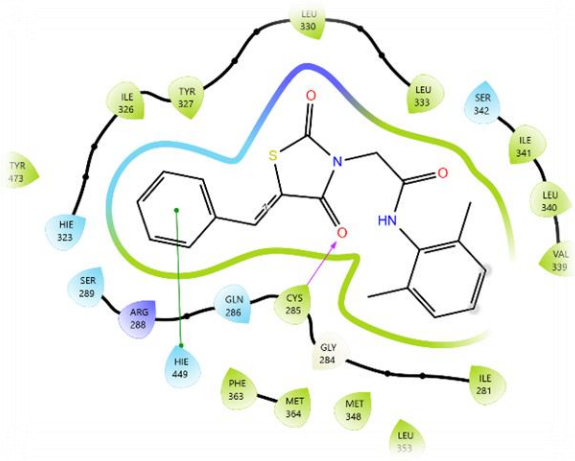

BTZD-11

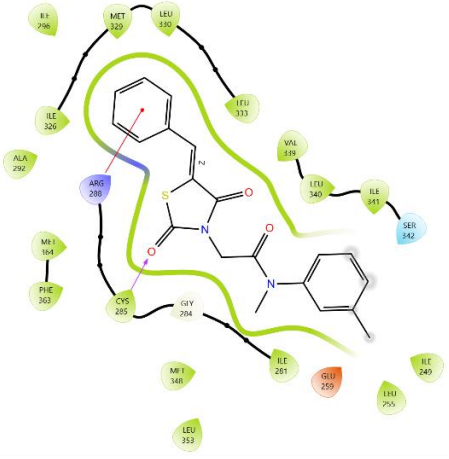

BTZD-12

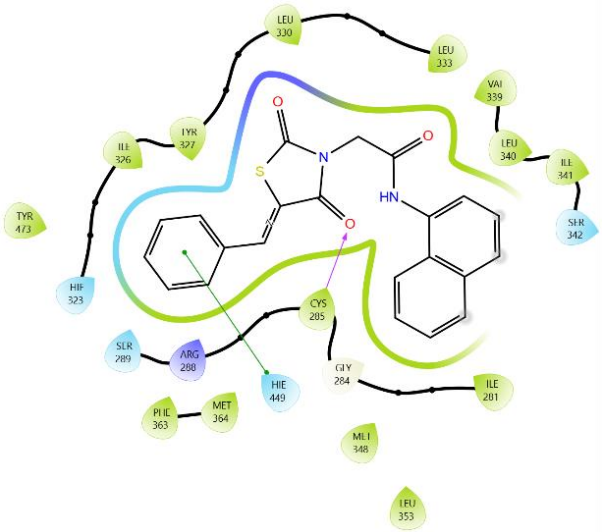

BTZD-13

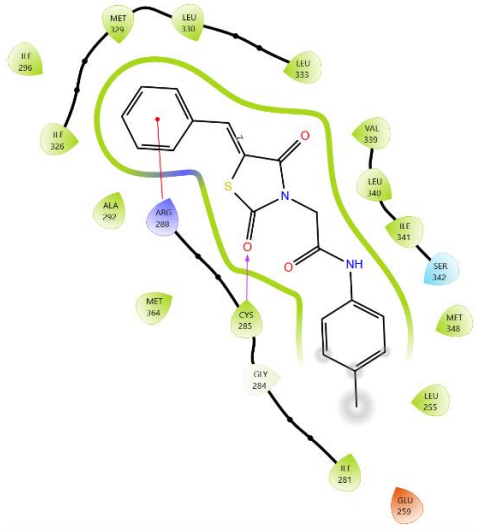

BTZD-14

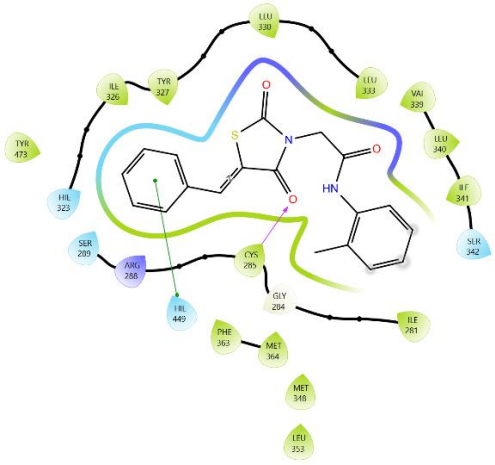

BTZD-15

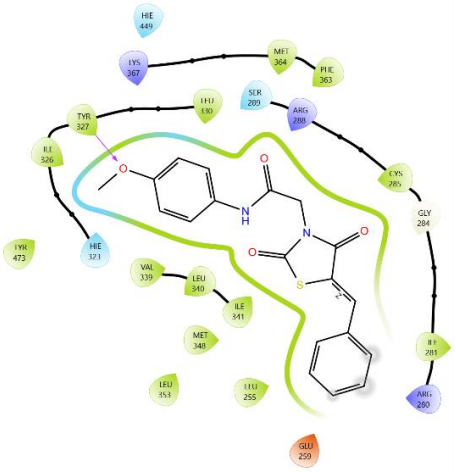

BTZD-16

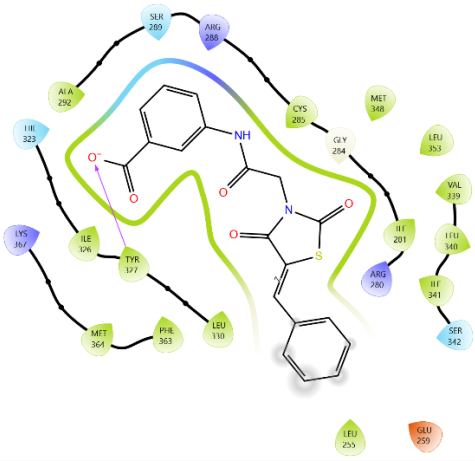

BTZD-17

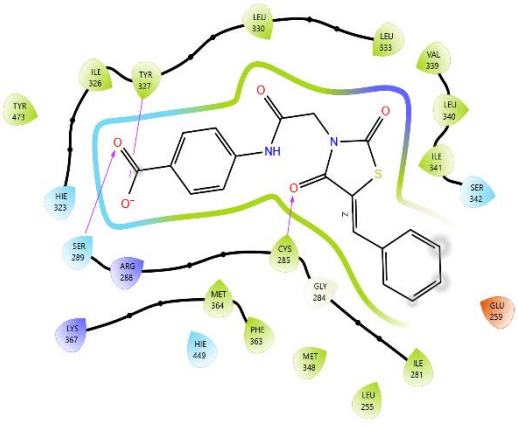

BTZD-18

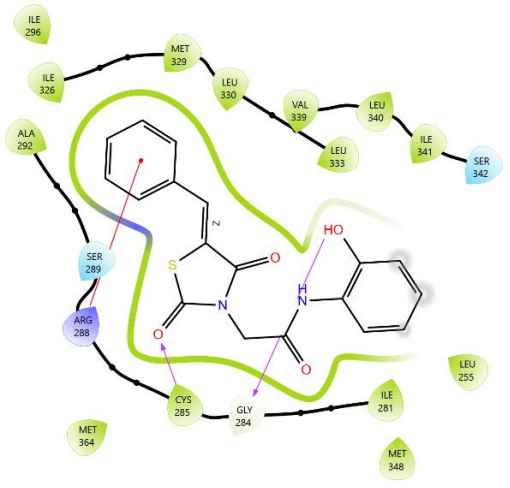

BTZD-19

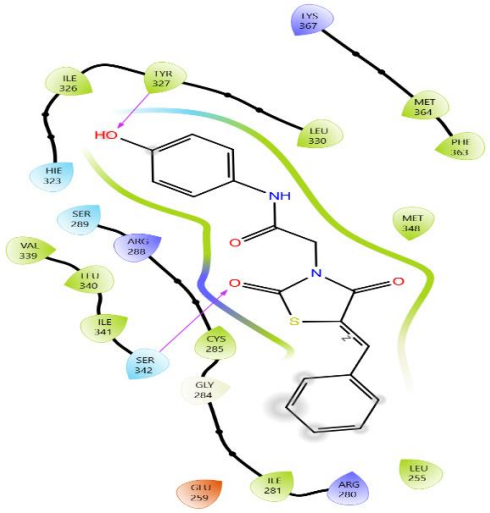

BTZD-20

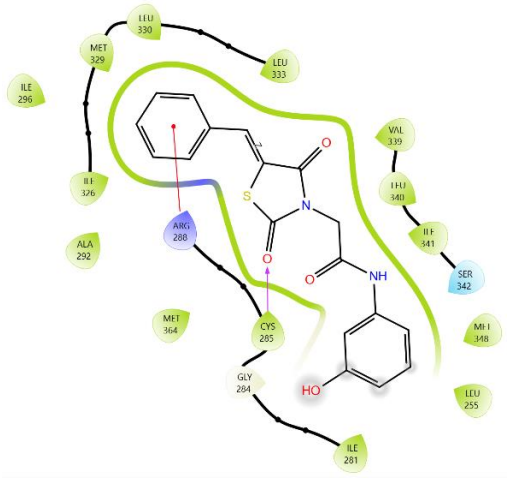

BTZD-21

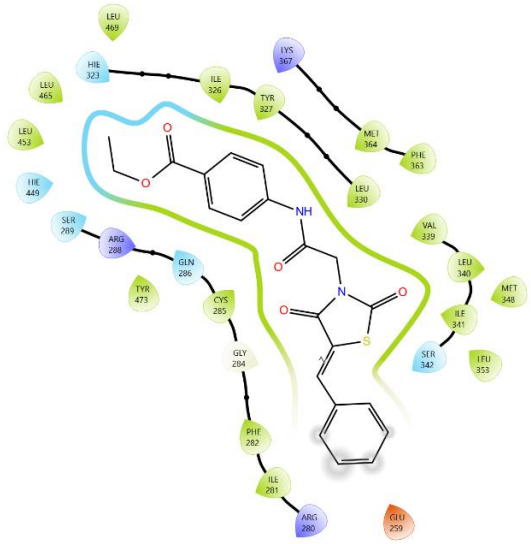

BTZD-22

Figure 4: 2D structure of binding interaction of receptor and compounds BTZD1 to BTZD22

Protein Preparation

Protein preparation is critical step before the molecular docking study. Protein preparation ensure that the use of protein in molecular studies is optimized and ready for the computational study. To begin, open the *Protein Preparation Wizard* in Maestro 24.3. The crystal structure of PPARδ (PDB ID: 5Y2O) was retrieved from the Protein Data Bank (PDB) (*www.rcsb.org*). The 5Y2O structure represents the ligand-binding domain of PPARδ in complex with pioglitazone. The structure was determined using X-ray diffraction with a resolution of 1.8 Å. The protein originates from *Homo sapiens* and was expressed in *E. coli*. This structure is illustrated in Figure 2.[17] Pre-process the protein structure by check the missing atom, deled the unwanted chains and water molecules and metals. Assign the correct bond order and add the missing hydrogen. Adjust the protonation state of amino acid (residue) based on pH (physiological pH=7). Minimize the energy of structure using the OPLS4 force field, ensuring the minimum distortion of original protein structure. Correct the issue steric clashes, improper torsions, or any irregularities using the editing tools in Maestro 24.3. once satisfied with prepared protein structure, saved the structure for docking studies.[18,19]

Quality Assessment of Prepared Protein

Quality of prepared 3D protein from protein preparation tools asses using the, Saves and ProSA web server before the molecular docking studies.[20]

Ligand Preparation

Ligand preparation was performed using the LigPrep tool in Maestro, a module from the Schrödinger Suite, is an essential step to generate a reliable 3D conformer with appropriate chemical and stereochemical properties for docking.[21] Load the molecular structures by import the Mol files of scaffold. Open the LigPrep panel in maestro for ligand preparation. Select all ligand imported and set the parameter in panel as tick on generate tautomer's, generate ionization states at default pH 2-7, generate stereoisomers and minimization of energy using the force field OPLS4.[18] We select the maximum 32 conforms per

structure. Run the job, after few minutes' ligand was prepared and saved in project table for further study.

Molecular Docking

Molecular docking studies in Maestro was conducted using Glide tool, a powerful docking module within the Schrödinger Suite. This tool enables the prediction of how small molecules interact with a target protein in terms of binding mode and strength. A key step in docking involves grid generation, which defines the ligand's binding site. To proceed, open the grid generation panel, locate the prepared protein structure, and specify the binding site by selecting the ligand base and clicking on any atom of the ligand. Finally, generate the grid and save the grid settings for docking study. Open the ligand docking panel in maestro and load the grid generated, import the prepared ligand file containing 22 molecules with additional cocrystal ligand. Choose the docking precision method, we selected high accuracy XP (Extra precision) method for ligand-receptor interaction. Run the docking and results saved in the project tables.[22]

Toxicity Prediction

Protox-III server used for the prediction of toxicity of individual molecules. Submit Smile structure of molecule into protox-III server with selection of type of toxicity.[23]

RESULT AND DISCUSSION

Design of 2,4-Thiazolidinedione Derivatives

The 2,4-thiazolidinedione (TZD) moiety is a diverse template with significant potential for chemical modification and the introduction of a wide variety of substituents. These modifications can be tailored to enhance biological activity, particularly for antidiabetic properties. Traditionally, TZD molecules are substituted at the tail region to optimize activity. However, recent studies suggest that N-substituted TZD derivatives exhibit promising antidiabetic activity by significantly lowering glucose levels. Incorporation of various acetamide derivatives at the nitrogen position of the TZD ring has shown to improve the efficacy of these molecules. By strategically altering the substituents on the TZD scaffold, researchers can optimize the pharmacokinetic and pharmacodynamic profiles of these compounds. This approach not only aims to improve efficacy but also to minimize side effects associated with existing antidiabetic therapies. Design of 2,4-thiazolidinedione with anti-diabetic properties were shown in Table-1.

Synthetic Accessibility Assay

The synthetic accessibility (SA) value is a valuable metric for assessing how easily a derivative can be prepared in the laboratory. This value score ranges from 1 to 10, where,1 indicates that the compound can be synthesized easily using well-known, straightforward procedures. 10 indicates that the compound is difficult to synthesize, requiring advanced skills and highly complex procedures. For the set of 22 compounds analyzed, the SA scores were found to fall within the range of 3 to 4, suggesting that these molecules are moderately easy to synthesize. This range indicates that while the synthesis may not be trivial, it is practical and achievable without requiring extremely specialized methods or resources. This level of synthetic accessibility is a positive sign, as it implies that these compounds can probably be produced on a practical scale for experimental testing or further refinement, making them promising candidates for research and use in medicinal chemistry.

ADME Analysis and Drug Likeness

The pharmacokinetic properties and pharmaceutical properties of 2,4-thiazolidineone derivatives evaluated by ADME tool in Maestro 24.3 and results in table no. 2 & 3. Most of the compound has oral absorption in the range of 82 to 100 % except BTZD-9, BTZD-17, BTZD-18. This indicates that the derivatives exhibit a high level of oral absorption. Predicated QPLogP o/w value of 22 derivatives are fall in the recommended range of -2.0 to 6.5 and QPlogBB is the predicated brain/blood partition coefficient of molecules and recommended range is -3.0 to 1.2 and most of the derivatives fall in recommended range except B-TZD-08 and B-TZD-09. These derivatives will not be cross the blood brain barrier and not adverse effect on CNS system. Metab denotes the predicted count of metabolic reactions for the 22 derivatives. with a recommended range of 1–8. QPlogS estimates water solubility, which refers to the concentration of solute that remains in equilibrium with its crystalline solid form in a saturated solution. The suggested QPlogS range falls between -6.5 and 0.5.

The pharmacokinetic properties and drug-likeness of 2,4-thiazolidinedione derivatives were evaluated using the ADME prediction tool in Maestro 24.3, and The findings are presented in Tables 2 and 3. The predicted oral absorption for most compounds ranged between 82% and 100%, indicating a high degree of oral bioavailability. Exceptions were observed for BTZD-9, BTZD-17, and BTZD-18, which exhibited slightly lower absorption levels. The lipophilicity QPLogP o/w values, representing the octanol-water partition coefficient, were within the recommended range of -2.0 to 6.5 for all 22 derivatives. This suggests that the compounds possess favourable lipophilicity for drug development.

The QPLogBB values, which estimate the brain-to-blood partition coefficient, mostly fell within the recommended range of -3.0 to 1.2. However, BTZD-08 and BTZD-09 exceeded this range, suggesting that these derivatives are unlikely to penetrate the blood-brain barrier. As a result, these compounds have a lower likelihood of causing adverse effects on the CNS. The predicted number of metabolic reactions for the 22 derivatives ranged from 1 to 8, aligning with the recommended values. This suggests that the compounds possess metabolic profiles suitable for further study.

The QPLogS values, representing the predicted Water solubility at saturation in balance with the crystalline solid phase, fell within the advised range of -6.5 to 0.5 for all derivatives. This suggests that the compounds possess adequate solubility and renal clearance, a critical parameter for drug development. These findings highlight the favourable ADME properties of the majority of the designed 2,4-thiazolidinedione derivatives, supporting their potential as drug candidates with good oral

absorption, acceptable metabolic stability, and limited CNS-related side effects.

Protein Preparation

The PPARδ receptor was chosen for docking studies. Its protein structure (PDB ID: 5Y2O) was retrieved from the Protein Data Bank (www.rcsb.org) and underwent a pre-processing step. This involved adding any missing atoms, removing unnecessary chains, water molecules, and metal ions, correcting bond orders, and adding missing hydrogen atoms. The protonation state of amino acid residues was adjusted to physiological pH (pH 7). The protein structure's energy was minimized using the OPLS4 force field to reduce structural distortions. This process corrected steric clashes and improper torsions.

Protein Structure Quality Assessment

The prepared protein was evaluated for quality using multiple analytical tools, like Ramachandran plot, ERRAT Graph, Verify 3D, ProSA and Plot of residue score. Quality check graph illustrated in Fig 3

Ramachandran Plot

The Ramachandran plot is the graph analysing protein backbone dihedral angles to ensure the majority of residue fall within allowed region.[24,25] The result of Ramachandran plot is 94% residue in favourable region shown in Fig 3(A).

ERRAT Graph

The ERRAT tool, commonly used in structural bioinformatics, evaluates protein structure quality by examining non-bonded atomic interactions. It assesses how well atoms that are not directly bonded interact, providing an overall measure of structural accuracy. The ERRAT score is represented as the percentage of the protein structure that falls within an acceptable threshold in Fig 3(B).[26] A higher ERRAT score of prepared protein is 98%, means that the majority of the protein's structure is well-constructed, suggesting that it is of high quality and suitable for further docking studies. This score indicates that the protein model is reliable for computational simulations of interactions with other molecules, like in drug discovery, where accurate protein structures are crucial for predicting binding outcomes.

Verify 3D Assay

The Verify 3D analysis evaluates a protein's structural accuracy by comparing it to its amino acid sequence. In this analysis, the X-axis represents specific residues, while the Y-axis denotes the corresponding quality score in Fig 3(C). A blue line indicates the average score across the sequence. The findings show that 92% of residues have a score exceeding 0.1, implying that the overall structural quality of the protein is well-preserved.

ProSA Study

ProSA-Web is a tool used to identify structural errors in both experimentally derived and computationally modeled proteins. It evaluates overall structural quality through a Z-score, where a more negative value reflects a higher-quality model. The ProSA analysis of this protein, with a Z-score of -8.89(Fig 3(D)), indicates strong reliability and a close resemblance to experimentally validated protein structures.

Plot of Residue Score

This graphical representation illustrates local model quality by mapping a knowledge-based energy function against residue order. Positive values suggest potential errors in the input structure or specific regions. To enhance clarity, the plot is smoothed by averaging energy values across 40-residue fragments, with the assigned value centered at i+19 (thick line) in Fig 3(D). A secondary thin line in the background provides a finer 10-residue window for additional detail. These results affirm the validity and reliability of the 3D structural model.

Molecular Docking Study

The docking study evaluates the efficacy of designed molecules by analyzing the interaction between 2,4-thiazolidinedione derivatives and the PPARδ receptor (PDB ID: 5Y2O).[17] As insulin sensitizers, these molecules activate PPARδ, potentially demonstrating antidiabetic properties. The docking score serves as a ranking parameter among the derivatives. Table 4 presents the docking scores of B-TZD1 to B-TZD22, ranging from -9.3 to -6.3. Among these, B-TZD11 and B-TZD13 exhibit favorable docking scores. The 2D visualization of these compounds' interactions with amino acid residues is depicted in Fig no. 4. The findings suggest that B-TZD11 engages in hydrophobic interactions with ILE326, TYR327, LEU330, LEU333, ILE341, LEU340, VAL339, PHE363, MET364, MET348, and LEU353. Additionally, it forms polar interactions with HIE323, SER289, GLN286, and SER342. ARG288 contributes to a positively charged interaction, while HIE449 participates in π-π interactions with the phenyl ring. Furthermore, CYS285 forms a hydrogen bond with the oxygen of the thiazolidinedione amide group. Similarly, B-TZD13 establishes hydrophobic interactions with ILE326, TYR327, LEU330, LEU333, VAL339, LEU340, ILE341, ILE281, MET348, LEU353, PHE363, MET364, and TYR473. It also engages in polar interactions with HIE323, SER289, and SER342, which are essential for enhancing the docking score. Like B-TZD11, B-TZD13 interacts with ARG288 through a positively charged interaction and participates in π-π electron interactions with HIE449. Moreover, the compound establishes a hydrogen bond with CYS285 via the oxygen of the thiazolidinedione moiety. Table 5 outlines the binding amino acid residues for these molecules. In general, the potential of these molecules to interact with amino acid residues in the binding region through non-bonded interactions enhances their binding affinity to the target protein, as demonstrated in the docking pattern.

In *Silico* Toxicity Prediction

The predicted toxicity analysis of the BTZD series offers detailed insights into the safety profile of these designed molecules. The toxicity predictions were assessed based on toxicity class, LD_{50} values, organ toxicity (hepato-, nephro-, and cardio-toxicity), and endpoint toxicity.

Predicted Toxicity Class and LD50 Values

All BTZD derivatives belong to toxicity class 4, indicating a moderate toxicity level. The predicted LD_{50} values range from 500 mg/kg to 1313 mg/kg, suggesting that these compounds exhibit varying degrees of acute toxicity. Notably, BTZD-17, BTZD-18, and BTZD-22 have the

lower LD_{50} values (500 mg/kg), implying higher acute toxicity compared to other derivatives, while BTZD-2 and BTZD-3 exhibit the highest LD_{50} (1313 mg/kg), indicating lower toxicity. The toxicity study results are presented in Table no.6

Organ Toxicity

Most BTZD compounds are projected to be inactive for nephrotoxicity, hepatotoxicity and cardiotoxicity, suggesting a low likelihood of causing severe organ damage. However, BTZD-1, BTZD-17, BTZD-18, BTZD-21, and BTZD-22 show nephrotoxicity, which may pose a potential risk for renal impairment. Among them, BTZD-1, BTZD-17, and BTZD-21 exhibit the highest nephrotoxic potential due to their additional endpoint toxicity.

End Point Toxicity

The BTZD derivatives exhibit varied endpoint toxicity profiles. Most compounds show inactivity against mutagenicity, immunotoxicity, cytotoxicity, and carcinogenicity, except for specific derivatives. Compounds BTZD-8 and BTZD-9 demonstrate activity towards the BBB barrier, carcinogenicity, and mutagenicity, while BTZD-17, BTZD-18, BTZD-19, and BTZD-20 exhibit an even broader endpoint toxicity spectrum, including cytotoxicity, mutagenicity, immunotoxicity, and carcinogenicity.

Blood-Brain Barrier (BBB) Penetration

Most compounds penetrate the BBB, which could be advantageous for central nervous system applications but requires careful evaluation to avoid neurotoxicity. Overall, while the BTZD derivatives exhibit promising biological interactions, their potential toxicity must be further evaluated through biological studies to ensure their safety and effectiveness.

CONCLUSION

The present study successfully designed and evaluated a series of 2,4-TZD molecules for their potential antidiabetic properties through molecular docking and in silico toxicity predictions. The synthetic accessibility assessment indicates that these derivatives are moderately easy to synthesize, making them viable candidates for further research. ADME analysis confirms favorable pharmacokinetic properties, including high oral absorption and adequate metabolic stability, with most compounds falling within recommended drug-likeness parameters. The docking studies reveal that B-TZD11 and B-TZD13 exhibit the most promising binding affinities to the PPARδ receptor, with key interactions that enhance their binding strength. These results support their potential as insulin sensitizers with antidiabetic activity. However, toxicity predictions indicate that while the majority of compounds belong to toxicity class 4 with moderate LD_{50} values, some derivatives, such as BTZD-17, BTZD-18, and BTZD-22, exhibit relatively higher acute toxicity. Organ toxicity assessments show that most compounds are non-toxic to major organs. End-point toxicity analysis further highlights that several compounds are inactive for mutagenicity, immunotoxicity, cytotoxicity, and carcinogenicity, while others exhibit potential BBB penetration, which may require further evaluation. Overall, the study provides a comprehensive in silico evaluation of the BTZD derivatives, highlighting their therapeutic potential as antidiabetic agents. Future biological validation, including animal and human clinical studies, is crucial to verify their efficacy and adverse effect profile for potential clinical use

Conflict of Interest

The authors affirm that they have no financial or personal conflicts of interest.

Acknowledgments

The authors sincerely appreciate the management of Schrödinger, LLC for granting access to the Maestro software suite 24.3, which played a crucial role in performing molecular docking and ADME analysis. Additionally, they extend their gratitude to Dr. Priyanka Banerjee of Protox for her contributions to the toxicity predictions in this study.

REFERENCES

1. Wolosowicz M, Prokopiuk S, Kaminski TW. Recent Advances in the Treatment of Insulin Resistance Targeting Molecular and Metabolic Pathways: Fighting a Losing Battle? *Medicina (Lithuania)*; 58. Epub ahead of print 1 April 2022. DOI: 10.3390/medicina58040472.
2. Nanjan MJ, Mohammed M, Prashantha Kumar BR, et al. Thiazolidinediones as antidiabetic agents: A critical review. *Bioorg Chem* 2018; 77:548–567.
3. Dadasaheb K, Jain N, Vijay J, et al. Design synthesis and evaluation of novel thiazolidinedione derivatives as antidiabetic agents. *Pharma Innov* 2017; 6:390–398.
4. Day C, Bailey CJ. Rosiglitazone☆. *Reference Module in Biomedical Sciences* 2016; 1–4.
5. Kobayashi M, Iwata M HT. Clinical evaluation of pioglitazone. *Nihon Rinsho* 2000; Feb:395–400.
6. Steven E. Nissen MD and KWM. Effect of Rosiglitazone on the Risk of Myocardial Infarction and Death from Cardiovascular Causes. *New England Journal of Medicine* 2007; 356:2457–71.
7. Lewis JD, Habel LA, Quesenberry CP, et al. Pioglitazone use and risk of bladder cancer and other common cancers in persons with diabetes. *JAMA - Journal of the American Medical Association* 2015; 314:265–277.
8. Wright MB, Bortolini M, Tadayyon M, et al. Minireview: Challenges and opportunities in development of ppar agonists. *Molecular Endocrinology* 2014; 28:1756–1768.
9. Sonawane G, Sharma S, Gilhotra R. In silico Analysis of 1,3,4-Oxadiazoles as Potential BCL-2 Inhibitor for Cancer Treatment. *Asian Journal of Chemistry* 2024; 36:1072–1088.
10. Patil K, Nemade M, Bedse A, et al. Virtual Screening, Molecular Docking, and ADMET Analysis of Flavonoids as a Potential Pi3k Inhibitor for Cancer Treatment. *International Journal of Drug Delivery Technology* 2023; 13:966–970.

11. Datar PA, Aher SB. Design and synthesis of novel thiazolidine-2 , 4- diones as hypoglycemic agents. *Journal of Saudi Chemical Society* 2016; 20:S196–S201.
12. Skoraczyński G, Kitlas M, Miasojedow B, et al. Critical assessment of synthetic accessibility scores in computer-assisted synthesis planning. *J Cheminform*; 15. Epub ahead of print 1 December 2023. DOI: 10.1186/s13321-023-00678-z.
13. Jorgensen WL, Duffy EM. Prediction of drug solubility from structure. *Adv Drug Deliv Rev* 2002; 54:355–366.
14. Lipinski CA, Lombardo F, Dominy BW, et al. Experimental and computational approaches to estimate solubility and permeability in drug discovery and development settings 1PII of original article: S0169-409X(96)00423-1. The article was originally published in Advanced Drug Delivery Reviews 23 (1997) 3–25. 1. *Adv Drug Deliv Rev* 2001; 46:3–26.
15. Jorgensen WL, Duffy EM. Prediction of drug solubility from Monte Carlo simulations. *Bioorg Med Chem Lett* 2000; 10:1155–1158.
16. Duffy EM, Jorgensen WL. Prediction of Properties from Simulations: Free Energies of Solvation in Hexadecane, Octanol, and Water. *J Am Chem Soc* 2000; 122:2878–2888.
17. Lee MA, Tan L, Yang H, et al. Structures of PPARγ complexed with lobeglitazone and pioglitazone reveal key determinants for the recognition of antidiabetic drugs. *Sci Rep* 2017; 7:16837.
18. Lu C, Wu C, Ghoreishi D, et al. OPLS4: Improving Force Field Accuracy on Challenging Regimes of Chemical Space. *J Chem Theory Comput* 2021; 17:4291–4300.
19. Madhavi Sastry G, Adzhigirey M, Day T, et al. Protein and ligand preparation: parameters, protocols, and influence on virtual screening enrichments. *J Comput Aided Mol Des* 2013; 27:221–234.
20. Wiederstein M, Sippl MJ. ProSA-web: interactive web service for the recognition of errors in three-dimensional structures of proteins. *Nucleic Acids Res* 2007; 35: W407–W410.
21. LigPrep. New York, NY: Schrödinger LLC, (2024).
22. Yang Y, Yao K, Repasky MP, et al. Efficient Exploration of Chemical Space with Docking and Deep Learning. *J Chem Theory Comput* 2021; 17:7106–7119.
23. Banerjee P, Kemmler E, Dunkel M, et al. ProTox 3.0: a webserver for the prediction of toxicity of chemicals. *Nucleic Acids Res* 2024; 52:W513–W520.
24. Laskowski RA, MacArthur MW, Thornton JM. PROCHECK: validation of protein-structure coordinates. Weily, 2012, pp. 684–687.
25. Laskowski RA, MacArthur MW, Moss DS, et al. PROCHECK: a program to check the stereochemical quality of protein structures. *J Appl Crystallogr* 1993; 26:283–291.
26. Colovos C, Yeates TO. Verification of protein structures: Patterns of nonbonded atomic interactions. *Protein Science* 1993; 2:1511–1519.